Interactive effects of temperature and nitrogen source on the elemental stoichiometry of a polar diatom

Nicolas Schiffrine, Jean-éric Tremblay, Marcel Babin

LIMNOLOGY and OCEANOGRAPHY

ASLO

Limnol. Oceanogr. 67, 2022, 2750–2762

doi: 10.1002/lno.12235

Interactive effects of temperature and nitrogen source on the elemental stoichiometry of a polar diatom

Nicolas Schiffrine [1,2*] **Jean-Éric Tremblay,** [1,2] **Marcel Babin** [2]

[1]Québec-Océan, Département de Biologie, Pavillon Alexandre-Vachon (Université Laval), Québec, Canada
[2]Takuvik Joint International Laboratory, CNRS (France) & Ulaval (Canada), Département de Biologie, Pavillon Alexandre-Vachon (Université Laval), Québec, Canada

Abstract

A recent study hypothesized that the near-zero temperatures that generally prevail in Arctic waters negate the influence that different nitrogen (N) sources can otherwise have on the growth and elemental stoichiometry of marine micro-algae. Here we test this hypothesis experimentally by evaluating how temperature (0–9°C) affects the growth and elemental stoichiometry of an ecologically relevant Arctic diatom *Chaetoceros gelidus* growing on different N sources (ammonium, nitrate, urea) at saturating irradiance. Following an initial acclimation period in which steady growth rates were achieved under each experimental treatment, changes in cellular concentrations of chlorophyll *a* and particulate carbon (C), nitrogen (N), phosphorus (P), and biogenic silica (Si) were monitored. While N source effects on growth rate became manifest as temperature rose above 0°C, the estimated optimal growth temperature was similar in all cases (T_{opt} = 8.3°C). A positive effect of temperature on the N : P ratio occurred only at 6°C. Above this temperature, the N : P ratio decreased to values close to those observed at 0°C and 3°C. By contrast, the C : N ratio remained nearly invariant between 0°C and 6°C but increased substantially at 9°C. Overall, the results suggest that the presently widespread and successful diatom *C. gelidus* possesses the ability to remain competitive despite ongoing environmental changes and that its responses to warming and the availability of different N sources may impact elemental fluxes in the future.

The Arctic region is warming two to three times faster than the global average rate (Meredith et al. 2019). This rapid pace has been attributed to the Arctic amplification, which includes the positive ice-albedo feedback and the increased penetration of warm Atlantic and Pacific waters at the periphery of the Arctic Ocean (Serreze and Barry 2011). Implications for the structure and function of marine ecosystems are likely to be profound since water temperature has a large influence on the metabolism, productivity, and spatial distribution of microbes (Eppley 1972; Raven and Geider 1988), with associated consequences on the biogeochemical cycling of elements and air–sea gas exchange.

Phytoplankton that thrive in polar oceans are considered to be adapted to low temperatures (Lyon and Mock 2014). While this adaptation suggests that polar diatoms should initially respond strongly and positively to modest warming, investigations of natural communities in the Barents Sea identified a ceiling temperature of 5°C, beyond which phytoplankton growth, biomass and net primary production are expected to decline (Holding et al. 2013; Coello-Camba et al. 2015; Coello-Camba and Agustí 2017). In addition, an experimental shift in temperature from 1.5°C (ambient) to 10°C led to the replacement of dominant diatoms by the pico-prasinophyte *Micromonas* and nanoflagellates in mesocosms experiments (Coello-Camba et al. 2015). Such changes in the relative contribution of different phytoplankton groups can have large implications for food webs and biogeochemistry since diatoms mediate a significant portion of carbon fluxes toward grazers and the deep ocean (Tréguer et al. 2018).

Warming can also affect biogeochemical fluxes by altering the elemental composition of microalgae, for example by modulating the amount of carbon (C) fixed and vertically exported per unit of the limiting nutrient (e.g., nitrogen, N) or modifying the nutritional value of organic matter for bacteria and grazers. According to the "temperature-dependent physiology" hypothesis (Toseland et al. 2013; Yvon-Durocher

*Correspondence: nicolas.schiffrine@takuvik.ulaval.ca

Additional Supporting Information may be found in the online version of this article.

Author Contribution Statement: N.S. designed the experiments, grew the cultures and conducted the analyses. N.S. and J.-É.T. wrote the manuscript with feedback from M.B.

et al. 2015), organisms growing at high temperatures should increase their N : P and C : P ratios due to a relatively low requirement for P-rich ribosomes relative to N-rich proteins. This response has been observed both in the laboratory (Toseland et al. 2013) and in a meta-analysis of field data (Yvon-Durocher et al. 2015). In the latter, N : P and C : P ratios of marine algae were best explained by latitudinal changes in average sea-surface temperature, with both ratios increasing 2.6-fold between 0°C and 30°C. Those analyses led to the hypothesis that ongoing ocean warming should drive the N : P and C : P ratios of marine organic matter upward. By contrast, predictions are difficult to formulate for the C : N ratio. Upon exposing eight taxonomically diverse species of temperate phytoplankton to temperatures ranging from 10°C to 25°C under saturating light conditions, Thompson et al. (1992) observed eight different growth responses. Some species exhibited a positive linear response and others showed a unimodal or weak negative trend.

While the literature on the photophysiological response of polar diatoms to temperature is extensive, relatively few studies examined how their elemental stoichiometry responds to changing growth conditions. In a recent study of the cosmopolitan Arctic diatom *Chaetoceros gelidus*, an ecologically relevant diatom that persists seasonally in the subsurface chlorophyll maximum (SCM), Schiffrine et al. (2020) found that cells growing on different N sources at 0°C had the same growth rates and elemental stoichiometry, contrasting with the results of prior studies performed on temperate species growing at relatively high temperatures. This novel observation was attributed to low temperature, which presumably nullifies the energy gain of using reduced N source due to a superseding limitation of growth rate by Rubisco activity. Here we aim to test the validity of this explanation by evaluating how temperature affects the growth and elemental stoichiometry of *C. gelidus* growing on different N sources at saturating irradiance. In doing so, we also aim to test the applicability of the results obtained by Schiffrine et al. (2020) at 0°C, which is typical of the SCM in the Beaufort Sea, to other sectors of the Arctic Ocean (e.g., the Barents Sea), where *C. gelidus* may be exposed to higher temperatures and rates of warming over time.

Materials and methods

Culture conditions

Strain RCC2046 of the Arctic diatom *C. gelidus* (Chamnansinp et al. 2013) was acquired from the Roscoff Culture Collection. Cultures were grown in sterile, acid- washed 0.5-L borosilicate Erlenmeyer flasks, with a working volume of 250 mL. The growth medium was prepared with an artificial seawater (ASW) base (Berges et al. 2001) and enriched with f/2 concentrations of silicate (106 μmol L^{-1} Si), trace metals and vitamins (Guillard 1975). Nitrogen was supplied as either NH_4^+, NO_3^- or urea as sole N source (100 μmol L^{-1} N). In order to approximate the nitrate to phosphate ratio observed in the coastal Beaufort Sea before the productive season begins, the concentration of phosphate in the medium was adjusted to obtain a nitrogen to phosphate ratio of 9 : 1 (11.11 μmol L^{-1} P) (Tremblay et al. 2008). All equipment used for medium preparation and culturing were previously soaked in 10% HCl during 48 h, then rinsed thoroughly with ultrapure, deionized water and finally autoclaved. Growth medium were sterilized by filtration (0.22-μm sterile filter; MediaKap-5; Repligen), thus avoiding potential issues of ion coprecipitation that can alter pH (*see* discussion in Berges et al. 2001). Cultures were illuminated continuously by Philips fluorescent tubes and attenuated by neutral-density screening (LEE filters: 216-White diffusion) to provide 200 μmol photons m^{-2} s^{-1}, which approximates the median irradiance in surface observed in the high Canadian Arctic across several regions (Martin et al. 2012). Triplicate cultures were maintained in semicontinuous growth and acclimated to a series of stepwise transfers to a range of temperatures including 0°C, 3°C, 6°C, and 9°C in a temperature-controlled growth chamber and mixed by gentle swirling each day (*see* Fig. S1 for more details). It should be noted that at 9°C, urea cultures crashed at the beginning of semicontinuous mode. In all cases, temperature in each culture was monitored continuously, with variation less than ±0.5°C. The analyses detailed below were performed on three subsamples in order to provide methodological replication for each harvest event. Note that the 0°C cultures were the focus of a parallel investigation of the joint effects of irradiance and N source on the growth and elemental composition of *C. gelidus* (Schiffrine et al. 2020).

Cell number, volume, and growth rate determination

Cell abundance and size (sphere-equivalent diameter) were monitored daily with a Multisizer 4 Coulter Counter (Coulter Counter Beckman) with a 25 μm aperture with an operational range of 4.034–20.16 μm. Both the lower and upper limits of the Coulter Counter were set according to the size range of *C. gelidus* (e.g., Chamnansinp et al. 2013). The instrument was routinely calibrated with 5 μm latex microspheres. Data blanks were generated with 0.2 μm filtered ASW. Samples were diluted (0.5 : 10) with 0.2 μm filtered ASW to meet instrument operational requirements. Three consecutive counts were achieved for each culture sampling point. Before and after each run, both the aperture tube and electrode were rinsed with distilled water and the aperture was flushed with ASW. Samples were bubbled before each count to break *C. gelidus* chains.

Growth rate was calculated as:

$$\mu = \ln(N_2/N_1)/(t_2 - t_1), \quad (1)$$

where N_2 is the cell concentration at time t_2 and N_1 is the cell concentration at time t_1. Mean cell size was calculated by multiplying bin diameter by the number of particles separately in

each bin, summing for the three bins, and dividing by the average particle count. Cell volume (equivalent spherical volume) was calculated from a spherical formula.

Chlorophyll *a* concentration

The concentration of chlorophyll *a* (Chl *a*), was determined by injecting 1 mL of culture directly into 6 mL of 90% acetone and incubating in the dark for 24 h at −20°C to extract pigments. The extracts were analyzed on a Turner TD-700 fluorometer (Turner Designs) based on the acidification method (Parsons et al. 1984). A blank was assessed by injecting 1 mL of artificial sea water into 6 mL of 90% acetone. The instrument was daily-calibrated with manufacturer-provided solid standard, and routinely calibrated with pure Chl *a* (C6144; Sigma-Aldrich).

Cellular content analysis

Samples for particulate organic carbon and total nitrogen (organic plus internal inorganic pools) were collected on precombusted Whatman GF/F filters, desiccated at 60°C and analyzed simultaneously using an elemental analyzer (ECS 4010; Costech Analytical Technologies, Inc.) coupled to a mass spectrometer (Delta V Advantage; Thermo-Finnigan). Samples for particulate phosphorus determination were filtered on precombusted Whatman filters, desiccated and oxidized using the method of Solórzano and Sharp (1980). Oxydized phosphorus (as PO_4^{3-}) was analyzed with standard colorimetric methods Hansen and Koroleff (2007) adapted for the AutoAnalyzer 3 (Bran + Luebbe). Samples for biogenic silicate determination were collected on 0.8-μm polycarbonate filters and frozen at −20°C. Filters were thawed in the laboratory and submitted to the alkaline hydrolysis method of Paasche (1980). The hydrolyzate was analyzed for $Si(OH)_4^-$ with an Autoanalyzer 3 (*see* above).

Description of relationships between growth and temperature

Thermal sensitivity of specific growth rate between pairs of experimental temperatures was evaluated by calculating the Q_{10} coefficient according to Eq. 2:

$$Q_{10} = (\mu_1/\mu_2)^{10/T_2 - T_1}, \quad (2)$$

where μ_1 and μ_2 are the specific growth rates at temperatures T_1 and T_2, respectively. Because the choice of T_1 and T_2 had an effect on Q_{10} values, calculations were made for three different temperature intervals between 0°C and T_{opt}. In parallel, the activation energy (E_a) was calculated by considering all experimental temperatures, using the nonlinear regression of Chen and Laws (2017) (Eq. 3):

$$\mu = \mu_0 \frac{e^{\frac{E_a}{k_b}\left(\frac{1}{T_0}-\frac{1}{T}\right)}}{1+\frac{E_a}{E_h-E_a}e^{\frac{E_h}{k_b}\left(\frac{1}{T_0}-\frac{1}{T}\right)}}, \quad (3)$$

where E_a (eV) is the activation energy of the growth rate without temperature inactivation, E_h (eV) is the parameter indicating how fast the growth rate decreases with increasing temperature due to high temperature inactivation, and T_0 is the reference temperature (273.15 K), T is the experimental temperature (°K), μ_0 is the growth rate constant at temperature T_0, T_{opt} (°K) is the optimal growth temperature, k is Boltzmann's constant (8.62×10^{-5} eV K^{-1}).

Data treatment, normalization, and statistical analysis

Cellular contents were normalized to cell concentration and cellular volume to yield cellular quotas (i.e., Q_X^C; pmol cell^{-1}) and volumetric quotas (i.e., Q_X^V; fmol μm^{-3}), respectively. Production rates of carbon and nitrogen (i.e., μQ_X^V; fmol μm^{-3} d^{-1}) were calculated by multiplication of the volumetric quota with the specific growth rate for each harvest event (i.e., S1, S2, S3 of the Step2D/3D in Fig. S1) of the respective treatment. Data are expressed as mean ± standard deviation (SD). Prior to statistical testing of differences between treatments, the normality of data distributions was checked and systematically rejected. Differences between treatments were assessed with a permutational multivariate ANOVA (PERMANOVA). Data analysis was performed with the *aovp* function of the *lmPerm* package in R and considered significant at $p < 0.05$.

Results

Thermal dependency of growth on different N sources

The growth rate (μ) of *C. gelidus* was highly influenced by temperature and N source, ranging from 0.26 to 0.65 d^{-1} across the different treatments (Fig. 1A). In the NH_4^+ cultures, the growth rate displayed a progressive 2.3-fold increase from 0°C to 6°C, while in the NO_3^- and urea cultures, the growth rate increased only between 3°C and 6°C (by 2.1- and 1.8-fold, respectively). The highest growth rate occurred at 6°C in all treatments and was significantly higher in the NH_4^+ and NO_3^- cultures (0.63 ± 0.05 d^{-1}) than in the urea culture (0.46 ± 0.02 d^{-1}; $p < 0.01$). At 9°C, the growth rate declined by ca. 40% in all N treatments and remained slightly higher in the NH_4^+ culture than in the other ones ($p < 0.05$). There was no clear pattern in cell volume across the temperature range for both NH_4^+ and NO_3^- cultures, for which the minimum and maximum cell volume occurred at 3°C and 6°C, respectively (Fig. 1B). Cell volume in the urea cultures decreased in a linear fashion between 0°C and 6°C (Fig. 1B).

Q_{10} values differed substantially depending on the temperature interval used for the calculation. Within the range of 0°C to 3°C, NH_4^+ cultures displayed higher Q_{10} values than

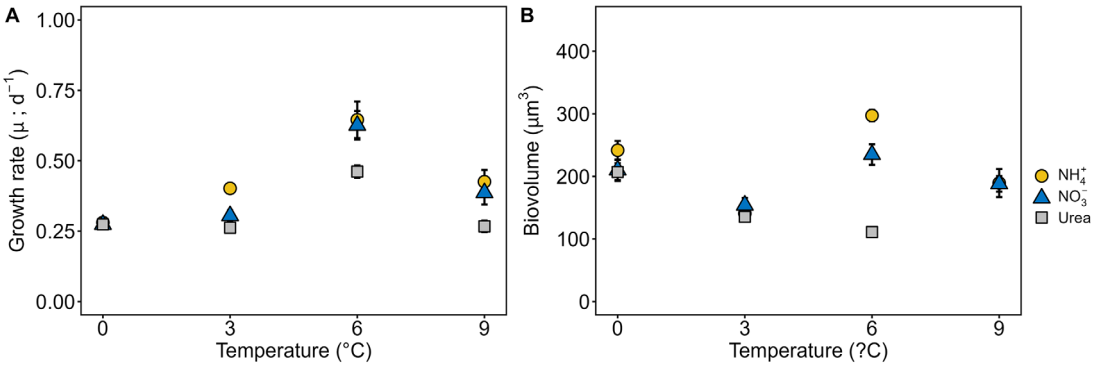

Fig. 1. Temperature dependence of growth rate (**A**) and cellular volume (**B**) for *Chaetoceros gelidus* acclimated across a range of temperature from 0°C to 9°C with NH_4^+ (yellow circle), NO_3^- (blue triangle) and urea (gray square) at saturating light. Values represent the means and error bars represent the standard deviation (i.e., SD) of triplicate samples.

NO_3^- and urea cultures (Table 1). In contrast, the Q_{10} values of NH_4^+ cultures were lower than those of NO_3^- and urea cultures between 3°C and 6°C (Table 1). Activation energies (E_a) were lower for the urea culture than for the NH_4^+ and NO_3^- cultures (Fig. S2; Table 1).

Elemental and Chl *a* volumetric quotas

Changes in cellular C, N, P, Si, and Chl *a* quota (Q_C^C, Q_N^C, Q_P^C, Q_{Si}^C, and $Q_{Chl\,a}^C$, respectively) in response to an increase in temperature with different N source were complex (Fig. 2A,C, E,G,I). Overall, urea cultures showed a decline in all cellular quotas (4–53%) as temperature increased, except for $Q_{Chl\,a}^C$ where no difference was observed between 3°C and 6°C (Fig. 2A,C,E,G,I). Changes in Q_C^C, Q_N^C, Q_{Si}^C, and $Q_{Chl\,a}^C$ presented a similar unimodal pattern across the temperature range, with the highest value were observed at 6°C (Fig. 2A,C, G,I), except for Q_P^C that was nearly invariant between 0 (0.03 ± 0.00 pmol P cell^{-1}) and 9°C (0.04 ± 0.01 pmol P cell^{-1}) (Fig. 2E). Across the entire temperature range, no significant differences were observed between NH_4^+ and NO_3^- cultures for both Q_C^C and Q_N^C ($p > 0.05$; Fig. 2A,C). From 0°C to 3°C, Q_C^C and Q_N^C decreased slightly (35% and 30%, respectively), then increased by 150% and 140% from 3°C to 6°C and decreased afterwards by 30% and 40%, respectively (Fig. 2A,C). For both NH_4^+ and NO_3^- cultures, warming from 0°C to 6°C induced a general increase in Q_{Si}^C (160% and 110%, respectively), followed by a similar decrease of 25% afterwards (Fig. 2G). Above 3°C, Q_{Si}^C was higher in the NH_4^+ cultures than in the NO_3^- cultures (Fig. 2G). In the NO_3^- cultures, $Q_{Chl\,a}^C$ displayed a progressive increase from 0°C to 6°C (97%; Fig. 2I), while in the NH_4^+ cultures, $Q_{Chl\,a}^C$ increased only between 3°C and 6°C (97%; Fig. 2I). Afterward, $Q_{Chl\,a}^C$ decreased by ca. 45% for both NH_4^+ and NO_3^- cultures (Fig. 2I). A significant difference in $Q_{Chl\,a}^C$ between the NH_4^+ and NO_3^- treatments was observed only at 3°C (Fig. 2I).

The volumetric quotas for C, N, P, Si, and Chl *a* (Q_C^V, Q_N^V, Q_P^V, Q_{Si}^V, and $Q_{Chl\,a}^V$, respectively) across the different N treatments were generally similar at 0°C ($p > 0.05$) but often diverged at higher temperatures (Fig. 2B,D,F,H,J). The Q_C^V of urea cultures increased more than twofold from 14.34 ± 2.77 to 31.15 ± 10.52 fmol C μm^{-3} between 0°C to 6°C (Fig. 2B). By contrast, Q_C^V in the other N treatments showed a negligible increase between 0°C and 3°C (Fig. 2B; $p > 0.05$), reaching relatively weak maxima at 6°C in the NO_3^- cultures (27.06 ± 11.47 fmol C μm^{-3}) and at 9°C in the NH_4^+ cultures (20.83 ± 6.97 fmol C μm^{-3}). Above 0°C, the NH_4^+ cultures exhibited lower Q_C^V than either the NO_3^- or urea cultures ($p < 0.05$).

In the urea cultures, warming induced an increase of Q_N^V from 0°C to 3°C but had no effect above this temperature (Fig. 2D). The value of 1.92 ± 0.31 fmol N μm^{-3} at 0°C was nearly half that at 3°C (3.66 ± 1.20 fmol N μm^{-3}) and 6°C (3.72 ± 1.02 fmol N μm^{-3}). In the NH_4^+ cultures, Q_N^V was constant from 0°C to 3°C (2.09 ± 0.24 fmol N μm^{-3}), increased a little at 6°C (2.50 ± 0.65 fmol N μm^{-3}) and decreased to an intermediate value at 9°C (2.23 ± 0.39 fmol N μm^{-3}) (Fig. 2D). There was a general rising trend in Q_N^V with warming in the NO_3^- cultures (Fig. 2D), with a minimum at 0°C (2.13 ± 0.29 fmol N μm^{-3}), a maximum at 6°C (3.67 ± 1.01 fmol N μm^{-3}) and an intermediate value at 9°C (2.71 ± 0.76 fmol N μm^{-3}). Above 0°C, Q_N^V was consistently lowest in the NH_4^+ cultures (Fig. 2D; $p < 0.05$).

The Q_P^V in the NO_3^- cultures was relatively constant from 0°C to 6°C (0.17 ± 0.02 fmol P μm^{-3}), followed by an increase

Table 1. Values of Q_{10} and activation energy (E_a, eV) for growth rate (μ, d^{-1}) of *Chaetoceros gelidus* growing on NH_4^+, NO_3^- or urea as sole N source. Numbers in parentheses indicate the standard deviation ($n > 9$).

	Q_{10}			
N treatment	[0;3]	[3;6]	[0;6]	E_a
NH_4^+	3.3 (0.4)	4.9 (1.3)	4.0 (0.7)	0.95
NO_3^-	1.5 (0.3)	11.1 (2.1)	4.0 (0.8)	1.10
Urea	0.9 (0.1)	6.7 (1.4)	2.4 (0.4)	0.69

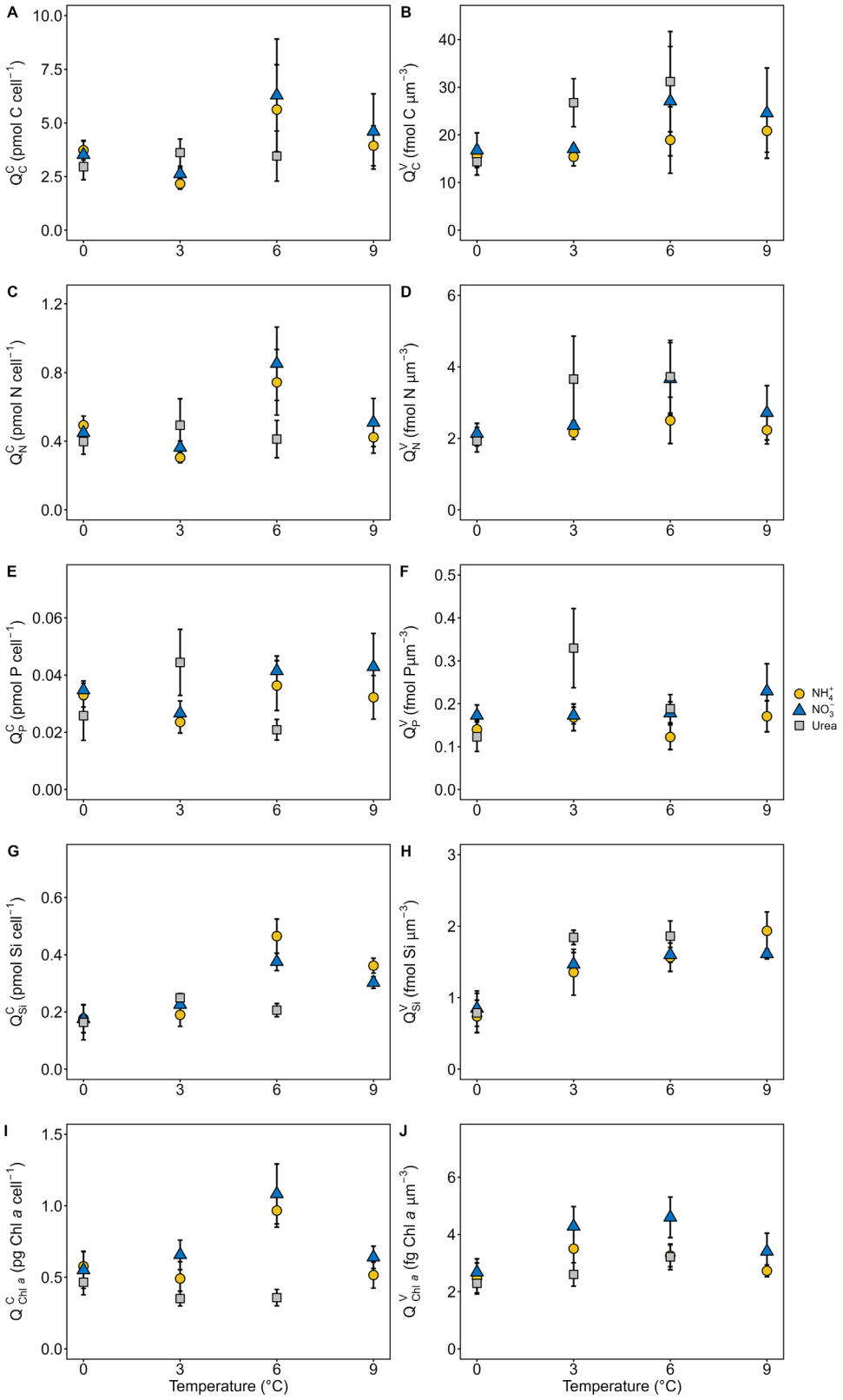

Fig. 2. Temperature dependence of cellular C (**A**), N (**C**), P (**E**), Si (**G**), and Chl *a* quota (**I**) and volumetric C (**B**), N (**D**), P (**F**), Si (**H**) and Chl *a* quota (**J**) for *Chaetoceros gelidus* acclimated across a range of temperature from 0°C to 9°C with NH_4^+ (yellow circle), NO_3^- (blue triangle) and urea (gray square) at saturating light ($n > 9$; mean ± SD).

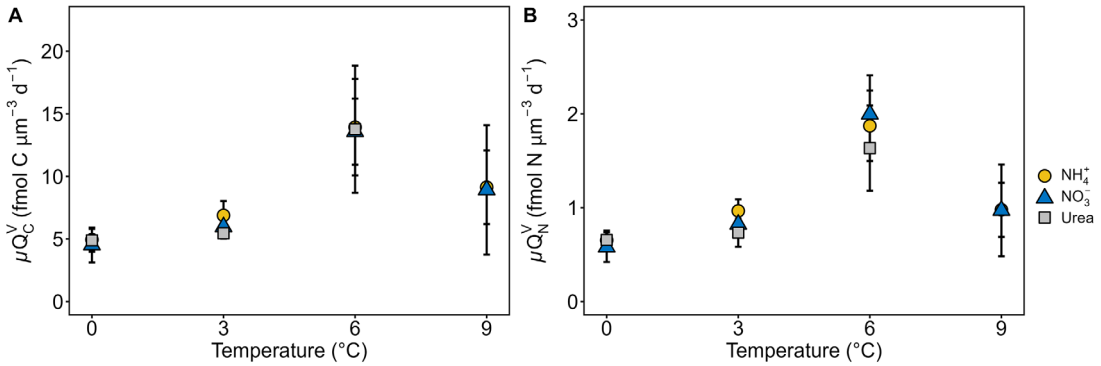

Fig. 3. Temperature dependence of production rate for C (**A**) an N (**B**) for *Chaetoceros gelidus* acclimated across a range of temperature from 0°C to 9°C with NH_4^+ (yellow circle), NO_3^- (blue triangle) and urea (gray square) at saturating light ($n > 9$; mean ± SD).

at 9°C (0.23 ± 0.06 fmol P μm^{-3}) (Fig. 2F). There was no clear pattern in the NH_4^+ cultures, for which the minimum and maximum Q_P^V occurred at 6°C (0.12 ± 0.03 fmol P μm^{-3}) and 9°C (0.17 ± 0.04 fmol P μm^{-3}), respectively (Fig. 2F). Urea cultures showed a sharp rise in Q_P^V from 0°C (0.12 ± 0.03 fmol P μm^{-3}) to 3°C (0.33 ± 0.09 fmol P μm^{-3}), followed by a decrease at 6°C (0.19 ± 0.03 fmol P μm^{-3}) (Fig. 2F). The NH_4^+ cultures had a lower Q_P^V than the other ones above 0°C, especially at 6°C and 9°C (Fig. 2F).

While the Q_{Si}^V increased linearly from 0 (0.79 ± 0.23 fmol Si μm^{-3}) to 9°C (1.93 ± 0.27 fmol Si μm^{-3}) in the NH_4^+ cultures (Fig. 2H), it reached a plateau at 6°C in the NO_3^- cultures (1.60 ± 0.10 fmol Si μm^{-3}). Except at 0°C, where no difference was observed between N treatments, Q_{Si}^V was consistently highest in the urea cultures (Fig. 2H). A significant difference in Q_{Si}^V between the NH_4^+ and NO_3^- treatments was observed only at 9°C (Fig. 2H).

Warming induced a general increase in $Q_{Chl\,a}^V$ in all N treatments, but the extent and shape of this increase varied considerably (Fig. 2j). Urea cultures showed a slight increase from 0°C (2.29 ± 0.33 fg Chl *a* μm^{-3}) to 6°C (3.25 ± 0.38 fg Chl *a* μm^{-3}), whereas the other treatments presented a bell-shaped curve with a maximum at 3°C in the NH_4^+ cultures (3.50 ± 0.90 fg Chl *a* μm^{-3}) and 6°C in the NO_3^- cultures (4.60 ± 0.71 fg Chl *a* μm^{-3}). At 3°C, 6°C, and 9°C, the NO_3^- cultures had a higher $Q_{Chl\,a}^V$ than the NH_4^+ and urea cultures (Fig. 2J; $p < 0.05$).

Throughout the temperature range, the production rate of C (i.e., μQ_C^V) was consistent across the different N sources ($p > 0.05$; Fig. 3A). The μQ_C^V of NH_4^+, NO_3^- and urea cultures displayed a progressive and similar 2.8-fold increase from 0°C to 6°C. At 9°C, μQ_C^V declined by ca. 35% in both NH_4^+ and NO_3^- cultures. The production rate of N (i.e., μQ_N^V) of NH_4^+ and NO_3^- cultures showed a general 1.5-fold increase between 0°C to 6°C and declined afterward to reach intermediate values (Fig. 3B). By contrast, μQ_N^V in urea cultures showed a negligible increase between 0°C and 3°C ($p > 0.05$) and reached a maximum at 6°C (Fig. 3B). Except at 0°C, where no difference was observed between N treatments, urea cultures exhibited lower μQ_N^V than either the NO_3^- or NH_4^+ cultures ($p < 0.05$). A significant difference in μQ_N^V between the NH_4^+ and NO_3^- treatments was observed only at 3°C (Fig. 3B).

Elemental stoichiometry

Both the NH_4^+ and NO_3^- cultures exhibited a relative decrease in molar C : N ratio from 0°C to 6°C, with minima of 7.39 ± 0.93 and 7.16 ± 1.36 mol C mol^{-1} N, respectively, followed by an increase to maximum values of 9.31 ± 0.76 and 8.82 ± 1.10 mol C mol^{-1} N, respectively, at 9°C (Table 2). By contrast, urea cultures displayed a general increase in C : N between 0°C (7.46 ± 1.01 mol C mol^{-1} N) and 6°C (8.25 ± 1.33 mol C mol^{-1} N). The C : N ratio did not statistically differ between NH_4^+ and NO_3^- cultures from 0°C to 6°C ($p < 0.05$) but was higher in the former at 9°C. The urea cultures had significantly lower ratios than the other two treatments at 3°C and 6°C (Table 2; $p < 0.05$). All the C : N ratios observed here were systematically higher than the canonical Redfield value of 6.62 mol C mol^{-1} N, irrespective of temperature and N source (Table 2).

The molar N : P ratios of NH_4^+ and NO_3^- cultures did not statistically differ ($p > 0.05$) and followed the same pattern with respect to temperature, with stable values at 0°C and 3°C, maxima at 6°C and minima at 9°C (Table 2). Urea cultures showed decreasing N : P between 0°C (16.19 ± 2.54 mol N mol^{-1} P) and 3°C (11.01 ± 1.25 mol N mol^{-1} P), followed by a maximum at 6°C (19.56 ± 3.78 mol N mol^{-1} P) (Table 2). For all N treatments, observed N : P ratios were lower than the canonical Redfield value of 16 mol N mol^{-1} P at 0°C, 3°C, and 9°C, but exceeded it by ca. 30% at 6°C (Table 2).

The molar Si : C ratio increased from 0°C to 3°C in all N treatments (Table 2), after which it either plateaued at 0.09 ± 0.02 mol Si mol^{-1} C (NH_4^+ cultures) and 0.06 ± 0.03 mol Si mol^{-1} C (urea cultures) or declined slightly (NO_3^- treatment) (Table 2). The molar Si : N ratio of NH_4^+ cultures showed a nearly linear increase from 0°C to 9°C (Table 2), whereas for NO_3^- cultures the increase occurred only from 0°C to 3°C and

Table 2. Molar C : N, N : P, C : P, Si : C, Si : N (mol mol^{-1}) ratios and C : Chl *a* (g g^{-1}) ratios of *Chaetoceros gelidus* acclimated to four different temperatures and growing on NH_4^+, NO_3^-, or urea as sole N source. Numbers in parentheses indicate the standard deviation ($n > 9$).

	Temperature	C : N	N : P	C : P	Si : C	Si : N	C : Chl *a*
NH_4^+	0	7.57 (0.59)	13.27 (1.15)	105.35 (6.02)	0.05 (0.01)	0.36 (0.09)	74.90 (10.3)
	3	7.10 (0.35)	13.74 (1.04)	93.16 (14.19)	0.09 (0.02)	0.63 (0.12)	55.12 (12.05)
	6	7.39 (0.93)	20.56 (3.28)	152.97 (35.4)	0.09 (0.02)	0.65 (0.11)	71.11 (27.11)
	9	9.31 (0.76)	13.17 (0.84)	122.20 (7.3)	0.10 (0.02)	0.89 (0.19)	76.82 (2.49)
NO_3^-	0	7.81 (0.98)	13.12 (1.15)	97.94 (19.02)	0.05 (0.02)	0.41 (0.13)	93.86 (24.01)
	3	7.24 (0.31)	13.74 (1.04)	99.57 (9.28)	0.09 (0.01)	0.62 (0.05)	48.66 (6.49)
	6	7.16 (1.36)	20.30 (3.04)	147.89 (46.39)	0.07 (0.03)	0.47 (0.13)	75.16 (39.89)
	9	8.82 (1.10)	11.97 (1.47)	105.50 (17.75)	0.07 (0.03)	0.63 (0.17)	57.56 (9.59)
Urea	0	7.46 (1.01)	16.19 (2.54)	112.82 (15.13)	0.05 (0.01)	0.35 (0.08)	84.83 (17.81)
	3	7.61 (1.14)	11.01 (1.25)	83.23 (11.05)	0.07 (0.01)	0.55 (0.16)	124.71 (24.08)
	6	8.25 (1.33)	19.56 (3.78)	161.74 (39.52)	0.07 (0.03)	0.53 (0.14)	119.98 (46.04)

was followed by a rough plateau between 3°C to 9°C (Table 2). In all experimental conditions both the Si : C and Si : N ratios were systematically lower than the Redfield-Brzezinski value (0.14 mol Si mol^{-1} C and 0.93 mol Si mol^{-1} N).

Temperature and N source had significant effects on the C : Chl *a* ratio. The NO_3^- culture showed a general decreasing trend in C : Chl *a* with increasing temperature, ranging from 93.86 ± 24.01 g Chl *a* g^{-1} C at 0°C to 57.56 ± 9.59 g Chl *a* g^{-1} C at 9°C, with a minimum at 3°C (48.66 ± 6.49 g Chl *a* g^{-1} C). The minimum ratio also occurred at 3°C in the NH_4^+ cultures (55.12 ± 12.05 g Chl *a* g^{-1} C), for which values were nearly invariant at other temperatures (ranging from 71.11 ± 27.11 to 76.82 ± 2.49 g Chl *a* g^{-1} C). In urea cultures, the C : Chl *a* ratio increased sharply from 0°C (84.83 ± 17.81 g Chl *a* g^{-1} C) to 3°C (124.71 ± 24.08 g Chl *a* g^{-1} C) and remained relatively even at 6°C. At 3°C, the high C : Chl *a* ratio observed in the urea cultures was more than twice higher than the values observed in the NH_4^+ and NO_3^- treatments.

Discussion

Thermal responses of *C. gelidus*

Temperature is important in regulating the diffusion and transport of nutrients, non-enzymatic and enzymatic reactions, as well as metabolic rates in phytoplankton (Raven and Geider 1988; Davison 1991). The response of phytoplankton growth to temperature typically follows a tolerance curve (Thomas et al. 2012; Boyd et al. 2013) in which growth rate increases up to T_{opt} and then decreases. The same pattern was observed for *C. gelidus* (Fig. 1), with an estimated T_{opt} of 8.3°C (i.e., 281.4 K; Fig. S2) similar to values observed for other polar *Chaetoceros* species but much lower than the values observed for temperate species of this genus (Table S1). These observations are consistent with the notion that cold-adapted polar phytoplankton have lower T_{opt} values than phytoplankton from lower latitudes (Thomas et al. 2012) and confirm that *C. gelidus* is psychrophilic (i.e., able to grow at temperatures below 15°C and exhibiting maximum growth rates at temperature optima below 18°C; Morgan-Kiss et al. 2006). This first estimate of T_{opt} should be considered as provisional since it is obtained by mathematical interpolation. Further experiments considering additional temperatures between 6°C and 9°C would improve accuracy. Beyond the T_{opt} estimated here, the growth rate of *C. gelidus* decreased sharply (Fig. S2), consistent with the results of Boyd et al. (2013) for the southern polar diatom *Proboscia inermis*, for which a 1°C increment above T_{opt} caused a drastic decrease in μ followed by mortality.

The temperature dependence of growth rate or specific chemical and biological processes is frequently described using the Q_{10} coefficient (Eppley 1972). Prior compilations of maximal growth rates using a larger number of species have found a Q10 of 1.88 (Eppley 1972). For *C. gelidus*, Q_{10} values ranged from 0.9 ± 0.1 to 11.1 ± 2.1 (Table 1), which is higher than the typical value for phytoplankton as suggested by Eppley (1972) but frequently observed in polar marine organisms (Hutchins and Boyd 2016; Zhu et al. 2016, 2017). Another commonly used descriptor of how fast growth rate increases with temperature is E_a (Chen and Laws 2017). The mean values of E_a observed (Table 1) are at the upper bound of values reported for other phytoplankton cultures isolated from 50°N to 75°N by Chen et al. (2014) (Fig. S3) and much higher than those determined for natural polar phytoplankton communities and polar phytoplankton cultures by Coello-Camba and Agustí (2017) (0.61 ± 0.07 eV). For the latter, the relatively large difference observed could be due to the linear regression used by Coello-Camba and Agustí (2017), which can result in relatively low E_a estimates (e.g., Chen and Laws 2017). The relatively high E_a values estimated in the present study suggest that *C. gelidus* is particularly responsive to warming.

Comparison of the element contents between *C. gelidus* and those of other polar or temperate diatoms

The comparison of observed elemental contents on a per cell basis with the literature shows intriguing results.

Remarkably, values of Q_C^C and Q_N^C in *C. gelidus* were lower than those reported by Lomas and Krause (2019) for diatom strains isolated from polar waters and grown at high light prior to harvest in mid-exponential growth phase. For example, the polar diatoms *Thalassiosira aestivalis*, *T. antarctica*, and *T. gravida* exhibit Q_C^C and Q_N^C up to, respectively, ca. 11 and 14 times higher than those observed for *C. gelidus* here. However, comparisons made on a per cell basis are limited since they do not account for differences in cellular volume. A comparison with recently published data describing the relationships between elemental contents on a per cell basis and cellular volume (e.g., Lomas et al. 2019) shows that *C. gelidus* stands out with respect to other polar diatoms (Fig. S4). In fact, the volumetric quotas of *C. gelidus* falls midway between those of Arctic and temperate species (Fig. S4). This intriguing observation suggests that, despite the psychrophilic character of this species, *C. gelidus* may be considered as an amalgam of polar and temperate traits (Schiffrine et al. 2020).

Moreover, Lomas et al. (2019) proposed that polar diatoms have higher volumetric quotas than temperate diatoms. Here we show with *C. gelidus* that this observation not only applies to very cold temperatures (0–2°C) but that all volumetric quotas except Q_P^V increase substantially with temperature up to 9°C (Fig. 2B,D,F,H,J). This pattern suggests that the contrast with temperate species is not primarily a function of growth temperature and is linked to a more fundamental difference in adaptation. Otherwise, the volumetric quotas of polar species would decline with rising temperature. The effect of temperature on Q_{Si}^V was particularly strong and possibly offers an explanation for the relatively low Si : N ratios of Arctic diatoms with respect to their Southern Ocean counterparts, especially at the polar front (*see* Schiffrine et al. 2020 for a discussion) where mean temperatures are relatively high (Freeman et al. 2016).

Does warming increase the energetic benefit of using reduced N sources?

Prior studies of the response of temperate phytoplankton to different N sources indicate that cells obtain a growth advantage and maximize C acquisition when growing on reduced N (e.g., Shi et al. 2015). Recently, Schiffrine et al. (2020) observed that *C. gelidus* growing at 0°C, did not exhibit enhanced growth or elevated cellular C quotas when exposed to NH_4^+ as sole N source. Here, we observed that when temperature rises above 0°C, the effects of N source on growth rate and elemental volumetric quotas become manifest (Figs. 1, 2). The fact that the production rate of C was lowest and equal in the NH_4^+ and NO_3^- cultures at 0°C and then increased linearly with temperature up to 6°C reinforces the notion that C fixation was severely constrained at low temperature (Fig. 3A). While warming partly alleviated this constraint at 3°C for NH_4^+-grown cultures (Fig. 3A), the growth rate of NO_3^- cultures did not change between 0°C and 3°C (Fig. 1). The fact that in NO_3^- cultures the production rate of N increased only slightly from 0°C to 3°C (i.e., 45%; Fig. 3B) and was lower than the production rate of N in NH_4^+ cultures at 3°C, suggests that the activity of nitrate reductase (NR), which is the first and key regulatory step in NO_3^- assimilation (Lomas and Glibert 2000; Gao et al. 2001), increased at a low pace relative to the activity of glutamate synthase, which is the enzyme mediating NH_4^+ assimilation (Glibert et al. 2016). At 6°C, the growth rate of *C. gelidus* did not significantly differ between the NH_4^+ and NO_3^- cultures (Fig. 1A), although the later showed 50% higher Q_C^V, Q_N^V and $Q_{Chl\,a}^V$ than the former (Fig. 2B,D,J). This result suggests that *C. gelidus* may have increased the production photosystem components (including pigments) to capture more light energy since the latter contain a significant portion of total cellular nitrogen and carbon (Li et al. 2015). This response would compensate for the greater energy cost of using NO_3^- through greater generation of reducing power. This observation contrasts with previous reports that temperate phytoplankton grown at or close to T_{opt} should exhibit lower growth rates and cellular quotas of C and N when using NO_3^- (Levasseur et al. 1993; Shi et al. 2015). While the growth rates of both the NH_4^+ and NO_3^- cultures decreased in a similar manner from 6°C to 9°C (−40%), NH_4^+ cultures maintained a slightly higher (+9%) growth rate than the NO_3^- cultures (Fig. 1A), possibly due to a greater thermal sensitivity of NR relative to glutamate synthase (Priscu et al. 1989; Gao et al. 1993). Overall, our data suggest that N source has no effect on N assimilation and C fixation but only on the growth rate and consequently on resource allocation at low and high temperatures.

Contrary to expectations that the energy benefit of using reduced N should be similar for urea and NH_4^+ (Antia et al. 1975), growth rate was consistently lower in the urea cultures than in the NH_4^+ and NO_3^- cultures between 3°C to 9°C (Fig. 1). Despite this difference, cells growing on urea between 3°C and 6°C had the highest volumetric elemental quotas and the lowest Chl *a* quotas (Fig. 2), whereas assimilation rates of C were relatively similar across N treatments (Fig. 3A). The slightly reduced rates of N incorporation in urea cultures (Fig. 3B) suggests that the assimilation of NH_4^+ derived from the urease-mediated cleavage of urea would probably be limited. While previous laboratory and field observations both suggest that the uptake of urea-N is positively related to temperature (Lomas and Glibert 1999; Spackeen et al. 2017), the provision of constant irradiance can severely depress urease activity (Bender et al. 2012). Collectively, these results suggest that cells growing on urea at 3°C and 6°C accumulated relatively large internal pools of C, N, and P but that the conversion of these pools into growth machinery and light-harvesting capacity (e.g., Chl *a*) was less complete than in the NO_3^- and NH_4^+ grown cells. As proposed by Collier et al. (2012), it would seem that the nutritional value of different N source is not simply an inverse function of their oxidation state.

Temperature-driven changes in elemental ratios

Several recent efforts have been made to elucidate the effect of temperature on the elemental stoichiometry of phytoplankton (Toseland et al. 2013; Yvon-Durocher et al. 2015, 2017), but the subject is far from settled given the high variability observed across studies (Table S3). Since the impact of N sources on the elemental ratios of *C. gelidus* was relatively mild across the range of environmentally relevant temperatures considered here (Table 2), the data obtained for all N source at a given temperature were pooled prior to investigating temperature effects (Figs. S5, S6).

Several different patterns are observed in the literature regarding the effect of temperature on molar C : N ratios (Fig. S5A). In our study, the C : N ratio of *C. gelidus* remained relatively stable between 0°C and 6°C (~ 7.5 mol C mol^{-1} N; Fig. S5A) since Q_C^V and Q_N^V increased in concert (Fig. S6A,B). This trend contrasts with the results of Montagnes and Franklin (2001), who found no clear effect of temperature on either Q_C^V or Q_N^V in a host of temperate phytoplankton species grown under moderate irradiance below T_{opt}. Between 6°C and 9°C, however, C : N increased by 19% due to a large decrease in Q_N^V (−25%) relative to Q_C^V (−11%) (Fig. S5A, S6A,B). This is often attributed to heat stress and the detrimental effect it can have on growth rate by impairing enzyme function and the proteins involved in photosynthesis (e.g., Grimaud et al. 2017).

The rise in N : P and C : P ratios from relatively constant values in the 0–3°C range to strong maxima at 6°C (Fig. S5B, C) is consistent with the "temperature-dependent physiology" hypothesis (Toseland et al. 2013; Yvon-Durocher et al. 2015) However, our results suggest that there are boundaries to the window of temperatures over which this hypothesis is valid. While Yvon-Durocher et al. (2017) tested only two temperatures corresponding to "ambient" and "warmer" conditions, we show here that the positive effect of temperature on N : P and C : P was manifest only at 6°C (i.e., the temperature treatment immediately preceding the estimated T_{opt}) since at 9°C the two ratios decreased to values that were close to those observed at 0°C and/or 3°C (Fig. S5B,C). The peak at 6°C was driven by concomitant elevations in Q_N^V and Q_C^V with no clear trend in Q_P^V (Fig. S6A–C), which might be due to an increase of the rate of P-rich ribosomes translation into N-rich proteins (Toseland et al. 2013). Our results imply that temperature effects on N : P and C : P ratios are mostly driven by changing C and N content and that the sign and magnitude of this change depend on where the experimental temperatures fall with respect to T_{opt}. This reasoning implies that the positive effect of temperature on N : P and C : P ratios should be greatest at T_{opt}, which would be worth testing in future studies.

While the observed increase in molar Si : C and Si : N ratios over the experimental temperature range used here is consistent with the literature (Fig. S5D,E; Table S3) mechanisms underlying those variations differ in *C. gelidus*. In our study, the change in Si : C and Si : N ratios was mostly explained by a differential increase in Q_{Si}^V instead of Q_C^V or Q_N^V (Fig. S6A,B, D). Several previous studies proposed that both polar and temperate diatoms build thicker frustules when their growth is limited by temperature and consequently exhibit elevated Si quotas (Paasche 1980; Stapleford and Smith 1996; Sheehan et al. 2020). By contrast, we observed that both Q_{Si}^V and cellular Si per cell surface (i.e., proxy of the degree of silicification of the cell wall; e.g., Paasche 1980) showed a positive linear increase with increasing temperature (Fig. S7), indicating that the frustule of *C. gelidus* thickened with warming. Although the same pattern was also observed for the southern diatom *Pseudo-nitzschia subcurvata* (Zhu et al. 2017), the reasons for this unexpected observation remain to be explored.

Implications for the current and future Arctic pelagic ecosystem

The current geographical distribution of *C. gelidus* has not been comprehensively established but available studies report high abundances in the Beaufort Sea, Baffin Bay, Davis Strait, and the Barents Sea. Molecular work has confirmed that the strains isolated from the Beaufort Sea and Barents Sea are genetically distinct from their temperate cousin *C. socialis* (Chamnansinp et al. 2013). Our data on the T_{opt} and thermal tolerance of *C. gelidus* imply that it is a cold-adapted, psychrophilic species. In the Beaufort Sea, *C. gelidus* is currently successful at temperatures that are much lower than its T_{opt} of 8.3°C (Figs. 1A, S2; Schiffrine et al. 2020). Water temperatures that are close to T_{opt} are only observed in the surface layer during late summer or in particularly shallow SCMs, whereas most of the SCM communities where *C. gelidus* thrives exist at near-zero temperatures. Collectively, our observations imply that *C. gelidus* is perfectly able to handle a considerable amount of warming that is unlikely to occur at the SCM for the foreseeable future. Even at 9°C, the growth rate remains substantially higher than at 0°C or 3°C.

It was recently proposed that nanophytoplankton and picoeukaryotes, such as *Micromonas*, will possibly replace diatoms in a warmer and more stratified future Artic Ocean (Li et al. 2009; Tremblay et al. 2009). It is highly doubtful, however, that *C. gelidus* will be outcompeted by other phytoplankton in the coastal waters where it currently dominates, since the maximum specific growth rates of *C. gelidus* reported here (μ_{opt} ranged from 0.46 ± 0.02 to 0.65 ± 0.07 d^{-1}) are among the highest ever reported in polar phytoplankton (Table S2). While this expectation has not been confirmed experimentally, it is compatible with recent on-deck incubations and laboratory studies in Baffin Bay, David Strait, and Kongsfjorden, in which *C. gelidus* along with *Thalassiosira* and *Micromonas* were the major components of the final phytoplankton assemblages under different temperatures and irradiance regimes (Hoppe et al. 2018).

Nitrogen is the primary liming nutrient over most of the Arctic Ocean (Tremblay and Gagnon 2009). We showed that *C. gelidus* is able to maintain relatively high growth rates on either NO_3^- or NH_4^+ at 0°C, 6°C, and 9°C, allowing it to be

successful under a wide range of conditions and nutrient supply pathways ranging from entirely allochthonous (e.g., NO_3^-) to regenerative (e.g., NH_4^+). It is noteworthy that at intermediate temperatures near 3°C, which are often observed in the upper euphotic zone and some particularly shallow SCM in late summer, *C. gelidus* has a relatively high potential for growth on NH_4^+ and a somewhat lesser capacity to grow on NO_3^- (Fig. 1). For urea above 0°C, this capacity is remarkably low despite the cell's ability to potentially accumulate large, uncharacterized pools of cellular C and N (Fig. 2A,B). This observation suggests that urea and possibly other sources of labile dissolved organic N would become less advantageous for diatoms as warming brings temperatures above those that typically characterize the SCM in today's Arctic Ocean.

The high C : N ratios observed at 9°C (Fig. S5A; Table 2) suggest that, per unit of the limiting nutrient, *C. gelidus* might potentially make a greater contribution to the vertical carbon pump at higher temperatures. This contribution would be strengthened by the positive relationship between temperature and the Si : C ratio, which imparts a greater ballasting effect and potential sinking rates under warm conditions. Because this relationship is accompanied by an increase in Si : N ratio that is primarily driven by Q_{Si}^V (Fig. S6D), warming can be expected to augment the contribution per unit N of *C. gelidus* to downward opal fluxes. This result raises the intriguing possibility that a warmer Arctic Ocean might retain a greater fraction of the silicate that transits from the Bering Sea to the Northwest Atlantic across the Pacific-influenced sector of the Arctic. The excess phosphate that follows the same pathway might also be reduced should warming eventually reach 6°C and enable the peak N : P ratio observed for *C. gelidus* at this temperature. At any other temperature, however, the N : P ratios of *C. gelidus* remain relatively low and typical of diatoms in general (Fig. S5B). Another intriguing hypothesis to test on other Arctic species is that the low N : P ratios obtained for diatoms in culture may only be valid for cells growing at temperatures below or above their T_{opt}. Finally, the relatively high C : N, Si : N, and Si : C ratios observed at high temperatures (Fig. S5A,C,D) suggest that the impact of *C. gelidus* on biogeochemistry is possibly different in the Barents Sea than in the Pacific-influenced sector of the Arctic Ocean. The highest Si : N ratios observed here also fall above prebloom silicate : nitrate ratios in the Barents Sea (ca. 0.47; e.g., Tremblay et al. 2015), which suggests that the growth and/or silification of *C. gelidus* likely experiences Si shortage in this sector of the Arctic Ocean. Low concentrations of dissolved iron in these waters and the adjacent Nansen Basin (e.g., Rijkenberg et al. 2018) possibly exacerbates Si shortage by increasing diatom demand for this nutrient (e.g., Meyerink et al. 2017).

Conclusions

This study is the first to show the combined effects of warming and N source on the growth and elemental stoichiometry of nutrient-replete, light-saturated cells of the widespread Arctic diatom *C. gelidus*. While the effects of N source become manifest as temperature rises and overarching constraints on C fixation are relaxed, this difference vanishes at 6°C, where cells using ammonium or nitrate grow equally well as temperature nears T_{opt}. At temperatures above 0°C, cells exposed to urea as sole N source have larger C and N quotas than those growing on either nitrate or ammonium but are unable to speed their growth at any other temperature than 6°C, where the growth increment remains relatively small. While natural phytoplankton communities take up urea in variable and sometimes high proportions with respect to other N sources in the Arctic (e.g., Simpson et al. 2013), our results suggest that doing so above 0°C under continuous light would be an impediment to growth when nitrate and ammonium are also available. It also suggests that a greater contribution of urea or other dissolved organic nitrogen sources to the total bioavailable N pool, which could result from greater vertical stratification and N recycling and/or the effect of permafrost thawing in peripheral drainage basins, might impede the growth of *C. gelidus* and other diatoms in a warmer Arctic Ocean.

The novel results reported here allow to propose new working hypotheses concerning the effect of temperature on elemental stoichiometry. Although our results support the conclusions of recent studies regarding the relationship between temperature and N : P and C : P ratios (Yvon-Durocher et al. 2015, 2017), we show that the positive effect of temperature on N : P and C : P ratios only below T_{opt} in *C. gelidus*. Therefore, knowing where experimental temperatures lay with respect to the T_{opt} for a given species appears crucial for understanding the responses of N : P and C : P ratios and to make informed predictions about the impact of warming on particular species or groups of phytoplankton.

Contrary to the notion that specific phytoplankton species are most successful in regions where mean annual temperatures are close to their T_{opt} (Boyd et al. 2013), it is apparent that *C. gelidus* generally thrives at temperatures well below its T_{opt}. Therefore, we formulate the hypothesis that some Arctic diatoms, such as *C. gelidus*, have the flexibility to be successful at much higher temperatures than those at which they typically grow and will not be easily outcompeted by temperate phytoplankton under realistic warming scenarios, especially at the SCM where stratification largely isolates the cells from surface warming. Finally, obtaining a detailed physiological characterization of ecologically relevant Arctic phytoplankton that make substantial contributions to surface blooms and subsequent primary production at the SCM seems essential to derive realistic modeling representations of future marine primary production and biogeochemical fluxes in the Arctic Ocean.

Data availability statement

The datasets generated for this study are available on request to the corresponding author.

References

Antia, N. J., B. R. Berland, D. J. Bonin, and S. Y. Maestrini. 1975. Comparative evaluation of certain organic and inorganic sources of nitrogen for phototrophic growth of marine microalgae. J. Mar. Biol. Assoc. U. K. **55**: 519–539. doi:10.1017/S0025315400017239

Bender, S. J., M. S. Parker, and E. V. Armbrust. 2012. Coupled effects of light and nitrogen source on the urea cycle and nitrogen metabolism over a diel cycle in the marine diatom *Thalassiosira pseudonana*. Protist **163**: 232–251. doi:10.1016/j.protis.2011.07.008

Berges, J. A., D. J. Franklin, and P. J. Harrison. 2001. Evolution of an artificial seawater medium: Improvements in enriched seawater, artificial water over the last two decades. J. Phycol. **37**: 1138–1145. doi:10.1046/j.1529-8817.2001.01052.x

Boyd, P. W., and others. 2013. Marine phytoplankton temperature versus growth responses from polar to tropical waters—Outcome of a scientific community-wide study. PLoS One **8**: e63091. doi:10.1371/journal.pone.0063091

Chamnansinp, A., Y. Li, N. Lundholm, and Ø. Moestrup. 2013. Global diversity of two widespread, colony-forming diatoms of the marine plankton, *Chaetoceros socialis* (syn. *C. radians*) and *Chaetoceros gelidus* sp. nov. J. Phycol. **49**: 1128–1141. doi:10.1111/jpy.12121

Chen, B., and E. A. Laws. 2017. Is there a difference of temperature sensitivity between marine phytoplankton and heterotrophs? Limnol. Oceanogr. **62**: 806–817. doi:10.1002/lno.10462

Chen, B., H. Liu, B. Huang, and J. Wang. 2014. Temperature effects on the growth rate of marine picoplankton. Mar. Ecol. Prog. Ser. **505**: 37–47. doi:10.3354/meps10773

Coello-Camba, A., and S. Agustí. 2017. Thermal thresholds of phytoplankton growth in polar waters and their consequences for a warming Polar Ocean. Front. Mar. Sci. **4**: 168. doi:10.3389/fmars.2017.00168

Coello-Camba, A., S. Agustí, D. Vaqué, J. Holding, J. M. Arrieta, P. Wassmann, and C. M. Duarte. 2015. Experimental assessment of temperature thresholds for Arctic phytoplankton communities. Estuaries Coasts **38**: 873–885. doi:10.1007/s12237-014-9849-7

Collier, J. L., R. Lovindeer, Y. Xi, J. C. Radway, and R. A. Armstrong. 2012. Differences in growth and physiology of marine *Synechococcus* (cyanobacteria) on nitrate versus ammonium are not determined solely by nitrogen source redox state. J. Phycol. **48**: 106–116. doi:10.1111/j.1529-8817.2011.01100.x

Davison, I. R. 1991. Environmental effects on algal photosynthesis: Temperature. J. Phycol. **27**: 2–8. doi:10.1111/j.0022-3646.1991.00002.x

Eppley, R. W. 1972. Temperature and phytoplankton growth in the sea. Fish. Bull. **70**: 1063–1085.

Freeman, N. M., N. S. Lovenduski, and P. R. Gent. 2016. Temporal variability in the Antarctic Polar Front (2002–2014). J. Geophys. Res.: Oceans **121**: 7263–7276. doi:10.1002/2016JC012145

Gao, Y., G. J. Smith, and R. S. Alberte. 1993. Nitrate reductase from the marine diatom *Skeletonema costatum* (biochemical and immunological characterization). Plant Physiol. **103**: 1437–1445. doi:10.1104/pp.103.4.1437

Gao, Y., G. J. Smith, and R. S. Alberte. 2001. Temperature dependence of nitrate reductase activity in marine phytoplankton: Biochemical analysis and ecological implications. J. Phycol. **36**: 304–313. doi:10.1046/j.1529-8817.2000.99195.x

Glibert, P. M., and others. 2016. Pluses and minuses of ammonium and nitrate uptake and assimilation by phytoplankton and implications for productivity and community composition, with emphasis on nitrogen-enriched conditions. Limnol. Oceanogr. **61**: 165–197. doi:10.1002/lno.10203

Grimaud, G. M., F. Mairet, A. Sciandra, and O. Bernard. 2017. Modeling the temperature effect on the specific growth rate of phytoplankton: A review. Rev. Environ. Sci. Biotechnol. **16**: 625–645. doi:10.1007/s11157-017-9443-0

Guillard, R. R. L. 1975. Culture of phytoplankton for feeding marine invertebrates, p. 29–60. *In* W. L. Smith and M. H. Chanley [eds.], Culture of marine invertebrate animals. Springer. doi:10.1007/978-1-4615-8714-9_3

Hansen, H. P., and F. Koroleff. 2007. Determination of nutrients, p. 159–228. *In* K. Grasshoff, K. Kremling, and M. Ehrhardt [eds.], Methods of seawater analysis. John Wiley & Sons. doi:10.1002/9783527613984.ch10

Holding, J. M., C. M. Duarte, J. M. Arrieta, R. Vaquer-Sunyer, A. Coello-Camba, P. Wassmann, and S. Agustí. 2013. Experimentally determined temperature thresholds for Arctic plankton community metabolism. Biogeosciences **10**: 357–370. doi:10.5194/bg-10-357-2013

Hoppe, C. J. M., K. K. E. Wolf, N. Schuback, P. D. Tortell, and B. Rost. 2018. Compensation of ocean acidification effects in Arctic phytoplankton assemblages. Nat. Clim. Change **8**: 529–533. doi:10.1038/s41558-018-0142-9

Hutchins, D. A., and P. W. Boyd. 2016. Marine phytoplankton and the changing ocean iron cycle. Nat. Clim. Change **6**: 1072–1079. doi:10.1038/nclimate3147

Levasseur, M., P. A. Thompson, and P. J. Harrison. 1993. Physiological acclimation of marine phytoplankton to different nitrogen sources. J. Phycol. **29**: 587–595. doi:10.1111/j.0022-3646.1993.00587.x

Li, W. K. W., F. A. McLaughlin, C. Lovejoy, and E. C. Carmack. 2009. Smallest algae thrive as the Arctic Ocean freshens. Science **326**: 539. doi:10.1126/science.1179798

Li, G., C. M. Brown, J. A. Jeans, N. A. Donaher, A. Mccarthy, and D. A. Campbell. 2015. The nitrogen costs of photosynthesis in a diatom under current and future pCO_2. New Phytol. **205**: 533–543. doi:10.1111/nph.13037

Lomas, M. W., and P. M. Glibert. 1999. Interactions between NH_4^+ and NO_3^- uptake and assimilation: Comparison of

diatoms and dinoflagellates at several growth temperatures. Mar. Biol. **133**: 541–551. doi:10.1007/s002270050494

Lomas, M. W., and P. M. Glibert. 2000. Comparisons of nitrate uptake, storage, and reduction in marine diatoms and flagellates. J. Phycol. **36**: 903–913. doi:10.1046/j.1529-8817.2000.99029.x

Lomas, M., and J. Krause. 2019. Elemental quotas and stoichiometry of polar diatoms, United States, Antarctica, Baffin Bay, and Norway, 2016-2018. 10.18739/A2D79596Q

Lomas, M. W., S. E. Baer, S. Acton, and J. W. Krause. 2019. Pumped up by the cold: Elemental quotas and stoichiometry of cold-water diatoms. Front. Mar. Sci. **6**: 286. doi:10.3389/fmars.2019.00286

Lyon, B. R., and T. Mock. 2014. Polar microalgae: New approaches towards understanding adaptations to an extreme and changing environment. Biology **3**: 56–80. doi:10.3390/biology3010056

Martin, J., J.-É. Tremblay, and N. M. Price. 2012. Nutritive and photosynthetic ecology of subsurface chlorophyll maxima in Canadian Arctic waters. Biogeosciences **9**: 5353–5371. doi:10.5194/bg-9-5353-2012

Meredith, M., and others. 2019. Polar regions. *In* H.-O. Pörtner and others. [eds.], IPCC Special Report on the Ocean and Cryosphere in a Changing Climate. Cambridge University Press.

Meyerink, S. W., M. J. Ellwood, W. A. Maher, G. D. Price, and R. F. Strzepek. 2017. Effects of iron limitation on silicon uptake kinetics and elemental stoichiometry in two Southern Ocean diatoms, *Eucampia antarctica* and *Proboscia inermis*, and the temperate diatom *Thalassiosira pseudonana*. Limnol. Oceanogr. **62**: 2445–2462. doi:10.1002/lno.10578

Montagnes, D. J. S., and M. Franklin. 2001. Effect of temperature on diatom volume, growth rate, and carbon and nitrogen content: Reconsidering some paradigms. Limnol. Oceanogr. **46**: 2008–2018. doi:10.4319/lo.2001.46.8.2008

Morgan-Kiss, R. M., J. C. Priscu, T. Pocock, L. Gudynaite-Savitch, and N. P. A. Huner. 2006. Adaptation and acclimation of photosynthetic microorganisms to permanently cold environments. Microbiol. Mol. Biol. Rev. **70**: 222–252. doi:10.1128/MMBR.70.1.222-252.2006

Paasche, E. 1980. Silicon content of five marine plankton diatom species measured with a rapid filter method. Limnol. Oceanogr. **25**: 474–480. doi:10.4319/lo.1980.25.3.0474

Parsons, T. R., Y. Maita, and C. M. Lalli. 1984. A manual of chemical & biological methods for seawater analysis. Elsevier.

Priscu, J. C., A. C. Palmisano, L. R. Priscu, and C. W. Sullivan. 1989. Temperature dependence of inorganic nitrogen uptake and assimilation in Antarctic Sea-ice microalgae. Polar Biol. **9**: 443–446. doi:10.1007/BF00443231

Raven, J. A., and R. J. Geider. 1988. Temperature and algal growth. New Phytol. **110**: 441–461. doi:10.1111/j.1469-8137.1988.tb00282.x

Rijkenberg, M. J. A., H. A. Slagter, M. R. van der Loeff, J. van Ooijen, and L. J. A. Gerringa. 2018. Dissolved Fe in the deep and upper Arctic Ocean with a focus on Fe limitation in the Nansen Basin. Front. Mar. Sci. **5**: 88. doi:10.3389/fmars.2018.00088

Schiffrine, N., J.-É. Tremblay, and M. Babin. 2020. Growth and elemental stoichiometry of the ecologically-relevant Arctic diatom *Chaetoceros gelidus*: A mix of polar and temperate. Front. Mar. Sci. **6**. doi:10.3389/fmars.2019.00790

Serreze, M. C., and R. G. Barry. 2011. Processes and impacts of Arctic amplification: A research synthesis. Glob. Planet. Change **77**: 85–96. doi:10.1016/j.gloplacha.2011.03.004

Sheehan, C. E., K. G. Baker, D. A. Nielsen, and K. Petrou. 2020. Temperatures above thermal optimum reduce cell growth and silica production while increasing cell volume and protein content in the diatom *Thalassiosira pseudonana*. Hydrobiologia **847**: 4233–4248. doi:10.1007/s10750-020-04408-6

Shi, D., W. Li, B. M. Hopkinson, H. Hong, D. Li, S.-J. Kao, and W. Lin. 2015. Interactive effects of light, nitrogen source, and carbon dioxide on energy metabolism in the diatom *Thalassiosira pseudonana*. Limnol. Oceanogr. **60**: 1805–1822. doi:10.1002/lno.10134

Simpson, K. G., J.-É. Tremblay, S. Brugel, and N. M. Price. 2013. Nutrient dynamics in the western Canadian Arctic. II. Estimates of new and regenerated production over the Mackenzie shelf and Cape Bathurst Polynya. Mar. Ecol. Prog. Ser. **484**: 47–62.

Solórzano, L., and J. H. Sharp. 1980. Determination of total dissolved phosphorus and particulate phosphorus in natural waters. Limnol. Oceanogr. **25**: 754–758. doi:10.4319/lo.1980.25.4.0754

Spackeen, J. L., and others. 2017. Interactive effects of elevated temperature and CO_2 on nitrate, urea, and dissolved inorganic carbon uptake by a coastal California, USA, microbial community. Mar. Ecol. Prog. Ser. **577**: 49–65. doi:10.3354/meps12243

Stapleford, L. S., and R. E. H. Smith. 1996. The interactive effects of temperature and silicon limitation on the psychrophilic ice diatom *Pseudonitszchia seriata*. Polar Biol. **16**: 589–594. doi:10.1007/BF02329056

Thomas, M. K., C. T. Kremer, C. A. Klausmeier, and E. Litchman. 2012. A global pattern of thermal adaptation in marine phytoplankton. Science **338**: 1085–1088. doi:10.1126/science.1224836

Thompson, P. A., M. Guo, and P. J. Harrison. 1992. Effects of variation in temperature. I. On the biochemical composition of eight species of marine phytoplankton. J. Phycol. **28**: 481–488. doi:10.1111/j.0022-3646.1992.00481.x

Toseland, A., and others. 2013. The impact of temperature on marine phytoplankton resource allocation and metabolism. Nat. Clim. Change **3**: 979–984. doi:10.1038/nclimate1989

Tréguer, P., and others. 2018. Influence of diatom diversity on the ocean biological carbon pump. Nat. Geosci. **11**: 27–37. doi:10.1038/s41561-017-0028-x

Tremblay, J.-É., and J. Gagnon. 2009. The effects of irradiance and nutrient supply on the productivity of Arctic waters: A

perspective on climate change, p. 73–93. *In* J. C. J. Nihoul and A. G. Kostianoy [eds.], Influence of climate change on the changing Arctic and sub-Arctic conditions. Springer. doi:10.1007/978-1-4020-9460-6_7

Tremblay, J.-É., K. Simpson, J. Martin, L. Miller, Y. Gratton, D. Barber, and N. M. Price. 2008. Vertical stability and the annual dynamics of nutrients and chlorophyll fluorescence in the coastal, Southeast Beaufort Sea. J. Geophys. Res. Oceans **113**. doi:10.1029/2007JC004547

Tremblay, G., C. Belzile, M. Gosselin, M. Poulin, S. Roy, and J.-É. Tremblay. 2009. Late summer phytoplankton distribution along a 3500 km transect in Canadian Arctic waters: Strong numerical dominance by picoeukaryotes. Aquat. Microb. Ecol. **54**: 55–70. doi:10.3354/ame01257

Tremblay, J.-É., L. G. Anderson, P. Matrai, P. Coupel, S. Bélanger, C. Michel, and M. Reigstad. 2015. Global and regional drivers of nutrient supply, primary production and CO_2 drawdown in the changing Arctic Ocean. Prog. Oceanogr. **139**: 171–196. doi:10.1016/j.pocean.2015.08.009

Yvon-Durocher, G., M. Dossena, M. Trimmer, G. Woodward, and A. P. Allen. 2015. Temperature and the biogeography of algal stoichiometry. Glob. Ecol. Biogeogr. **24**: 562–570. doi:10.1111/geb.12280

Yvon-Durocher, G., C.-E. Schaum, and M. Trimmer. 2017. The temperature dependence of phytoplankton stoichiometry: Investigating the roles of species sorting and local adaptation. Front. Microbiol. **8**: 2003. doi:10.3389/fmicb.2017.02003

Zhu, Z., K. Xu, F. Fu, J. Spackeen, D. Bronk, and D. Hutchins. 2016. A comparative study of iron and temperature interactive effects on diatoms and *Phaeocystis antarctica* from the Ross Sea, Antarctica. Mar. Ecol. Prog. Ser. **550**: 39–51. doi:10.3354/meps11732

Zhu, Z., P. Qu, J. Gale, F. Fu, and D. A. Hutchins. 2017. Individual and interactive effects of warming and CO_2 on *Pseudo-nitzschia subcurvata* and *Phaeocystis antarctica*, two dominant phytoplankton from the Ross Sea, Antarctica. Biogeosciences **14**: 5281–5295. doi:10.5194/bg-14-5281-2017

Acknowledgments

The authors are most grateful to Jonathan Gagnon and Gabrièle Deslongchamps for their assistance with cellular content analysis. We thank Flavienne Bruyant for her valuable help during the experiments. This work was supported financially and logistically by the Canada Excellence Research Chair (CERC) program, the strategic research cluster Quebec-Océan (Fonds de Recherche du Québec - Nature et Technologie) and by grants to J.-É. T. from the ArcticNet Network Center of Excellence and the National Sciences and Engineering Research Council of Canada (NSERC). It contributes to the scientific programs of Institut Nordique du Québec (INQ), Québec-Océan and the Takuvik Joint International Laboratory (UMI 3376) of Université Laval (Canada) and the Centre National de Recherche Scientifique (France).

Conflict of interest

None declared.

Submitted 19 April 2021
Revised 15 December 2021
Accepted 28 August 2022

Associate editor: Tatiana Rynearson